

Slip-links, hoops and tubes: tests of entanglement models of rubber elasticity

P. G. Higgs and R. J. Gaylord*

Cavendish Laboratory, Madingley Road, Cambridge CB3 0HE, UK

(Received 16 February 1989; revised 10 April 1989; accepted 8 May 1989)

A number of models of rubber elasticity are described in terms of their physics and then compared with experimental data. The models that are examined all assume that entanglements act along the entire contour length of a network chain, either discretely or in a mean field manner. The experiment that is used is the uniaxial extension-compression behaviour of several different networks. The mean field localization or random tube model and the discrete hoop model give the most satisfactory fit to the data.

(Keywords: rubber elasticity; modelling; entanglements)

INTRODUCTION

The number of theoretical models dealing with entanglement effects in rubber elasticity is large and continues to grow. In this paper we review the relative successes of some of these theories in fitting data from a range of crosslinked materials in uniaxial extension and compression. We assess the developments in theory which have occurred since the review of Gottlieb and Gaylord¹. We will not consider models which are purely phenomenological, or those whose physical content seems to us to be unreasonable. In particular, the constrained-junction fluctuation theory, although having considerable empirical success at data fitting, appears fundamentally misguided in attributing the effects of entanglement solely to the motion of the junctions and not at all to the chains themselves and therefore isolating the equilibrium elastic response of a network from the rubbery plateau response of its parent melt. We therefore will not examine this theory here. Rather, we look at models in which the constraining effects of entanglements on the lateral motion of chains is modelled by discrete slip-links, hoops, and by mean field localization effects modelled by tubes. We will discuss the physical differences between the models in the text. All necessary mathematical formulae are given in the Appendices.

In *Figure 1* we plot stress against strain for several data sets in a scaled form. The solid curve is the function $(\lambda - \lambda^{-2})$, the prediction of the simplest phantom chain theories of network elasticity. All the data can be scaled to fit almost exactly to the phantom chain theory for compression, whilst in extension a small but significant difference is apparent. It should be borne in mind in all that follows that the differences between the theories being compared are small compared with the absolute magnitude of the stresses, and that there is a surprising degree of uniformity of all the data sets considered. The Mooney-Rivlin plot (reduced stress $f^* = \sigma/(\lambda - \lambda^{-2})$ against λ^{-1}) emphasizes differences and therefore provides a better representation for assessing the predictions of the

models. However, it also emphasizes the scatter of the experimental points, particularly close to $\lambda = 1$. Finally, we should not place too great an importance on the theoretical fit with any one data set.

SLIP-LINK/HOOP MODELS

The viscoelasticity theory of Doi and Edwards² refers to both the ideas of slip-links and tubes. Marrucci³, and later Graessley⁴, applied the slip-link idea explicitly to trapped entanglements in crosslinked networks. The free energy (strain-dependent part only) may be written as equation (A1) in Appendix A. It has already been shown¹ that this Doi-Edwards-Marrucci-Graessley (DEMG) model provides a very poor representation of the data. Therefore, we will not plot the curve, but will only describe the concepts underlying this model for comparison to what follows.

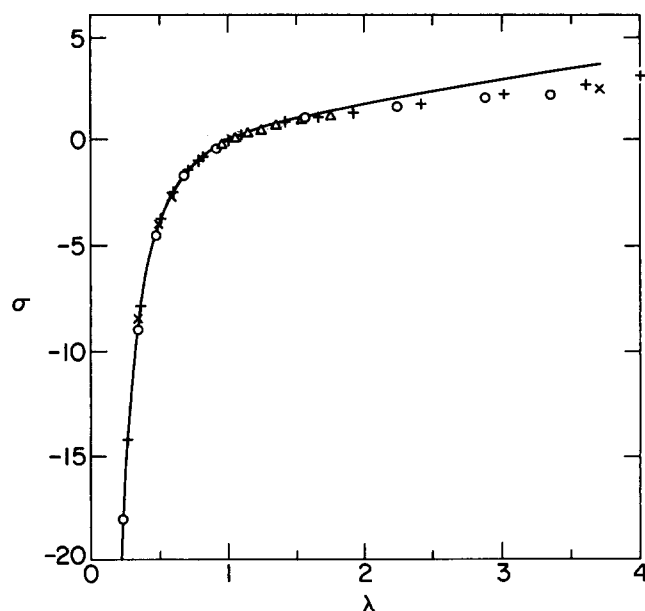


Figure 1 Stress-strain curves for several networks in uniaxial extension-compression, scaled to fit the Gaussian model stress-strain relation, $\sigma = \lambda - 1/\lambda^2$ (in kg cm^{-2}). \times , Natural rubber¹²; \circ , PDMS¹³; $+$, rubber (8% S)¹⁴; \triangle , PDMS¹⁵

* Permanent address and to whom correspondence should be addressed: Department of Materials Science and Engineering, University of Illinois, 1304 West Green Street, Urbana, IL 61801, USA

In the DEMG model a chain is divided into a fixed number of subchains by slip-links. The subchains are taken to deform affinely but the number of segments in each subchain varies with strain and is determined by requiring there to be equal tension in each subchain. Physically, the model applies the 'equilibration' process of Doi and Edwards² while suppressing chain end retraction.

The hoop model⁵ considers a chain crosslinked at its ends and divided into N subchains by $N-1$ hoops (or slip-links) representing trapped entanglements. Chain units are free to move through the hoops and redistribute themselves between the subchains so as to minimize the free energy of the total chain. The crosslinks and hoop positions are both assumed to deform affinely. The chemical potential for increasing the contour length of chain between each pair of hoops is calculated, and it is this quantity rather than the tension, which is taken to be constant at all points on the chain. The resulting free energy expression (equation (A2)) has two parameters, $a \sim Nv$ where v is the number of chains per unit volume, and $b \sim v$. Thus in a highly entangled network the second term becomes negligible with respect to the first. The product Nv is the total number of hoops per volume. It is assumed that adding crosslinks to the system does not appreciably change the degree of entanglement, so that a remains independent of crosslink density and thus N varies inversely with v . The number of hoops per unit length along any one chain is proportional to the segment density ρ , and since the total contour length per unit volume is ρ , $a \sim \rho^2$, i.e. a is proportional to the plateau modulus of the uncrosslinked system.

If the contour length in each subchain is constrained to be its most probable value then the hoop model becomes the DEMG model and equation (A2) reduces to equation (A1). It is the fluctuations about this value that produce the extra terms appearing in equation (A2). We note that the case $N=2$ corresponds to the Kosc model⁶. The derivation of Adolf⁷ attempts the same general N case as Higgs and Ball⁵, but incorporates pre-averaging simplifications which severely affect the final answer given in equation (A3) (in particular the affine deformation function terms $\langle M^2 \rangle$ and $\langle M \rangle^2$ defined in Appendix B become indistinguishable). Such differences are crucial in determining the shape of the stress-strain curve. We therefore do not use the Adolf model equation (A3) but instead use the more exact hoop model equation (A2) for fitting the data.

The replica slip-link model⁸ considers one very long chain which is crosslinked to itself N_c times and which is linked to itself via slip-links N_s times. This chain represents the whole network, i.e. the ends of the individual chains in a real network are assumed to be unimportant. Slip-links may slide freely some distance up and down the network chains. This distance is characterized by the slippage parameter η . The replica formalism is used to calculate the free energy by considering all configurations of the network consistent with one arrangement of the slip-link points, and subsequently averaging the result over all ways of arranging the slip-link points along the contour of the original long chain. It thus avoids having to assume an affine deformation of the slip-link points. There is an important difference between a slip-link of the replica slip-link model, which is not fixed in space and only affects two network chains and a hoop of the hoop model,

which is fixed in space and which represents the constraints of all of the other network chains on the single network chain being considered.

The free energy of the replica model (equation (A4)) is a sum of crosslink and entanglement terms. The entanglement contribution is a function of the slippage parameter η . A separate theoretical analysis⁸ based on free energy minimization estimates η to be approximately 0.234. Edwards and Vilgis⁹ have given a 'Flory segment' argument for the slip-link free energy. They show that this single chain approach, which has some similarity to the hoop model⁵, can be tailored to match the replica result equation (A4) at small strains.

The data points in Figures 2 and 3 are the same as in Figure 1 plotted in the Mooney-Rivlin form using the same scaling factors. Therefore the data should pass as closely as possible through the point $f^* = 1$ at $\lambda^{-1} = 1$. The theory curves are the least squares fits to the data on natural rubber¹². Due to the close coincidence of the data sets there is no significant difference in the plots if best fits to another data set are shown instead.

The hoop model fits the flatter Mooney-Rivlin curve in compression much better than the replica slip-link model, whilst the replica model is slightly better in extension. The fitting parameters and the mean square

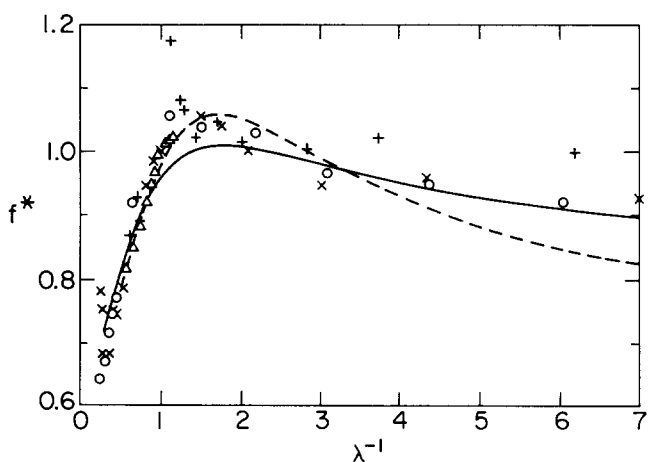


Figure 2 Data from Figure 1 plotted in the Mooney-Rivlin form. Curves are best fits to the natural rubber network (\times). Theoretical curves are for: —, Hoop model (equation (A2)); ----, replica slip-link model (equation (A4)). See Table 1 for fitting parameters and their best-fit values (f^* units are kg cm^{-2})

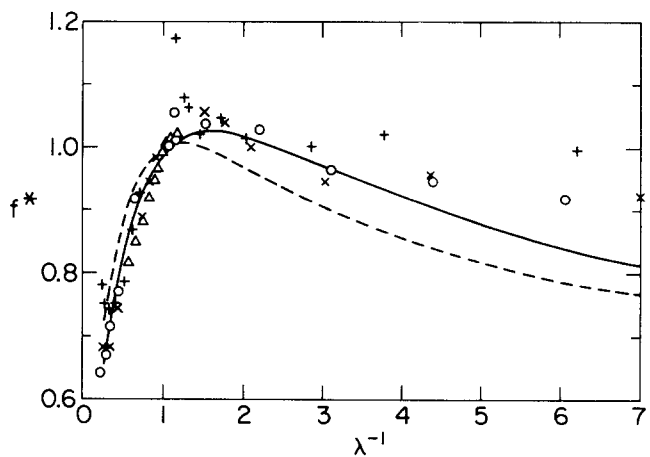


Figure 3 Data from Figure 2. Theory curves are for: —, random tube or localization model (equation (A5)); ----, straight tube model (equation (A7)). See Table 1 for fitting parameters and their best-fit values (f^* units are kg cm^{-2})

Table 1 Best-fit parameter values used in Figures 2 and 3

Model	Parameters	Natural rubber ¹²			PDMS ¹³		
		<i>b/a</i>	η	$10^3 \times \Delta^2 \dagger$	<i>b/a</i>	η	$10^3 \times \Delta^2$
Hoop (A2)	<i>a, b</i>	0.0*	–	4.3	–	–	2.0
Replica slip-link (A4)	<i>a, b, \eta</i>	0.66	0.82	5.5	0.65	0.64	1.8
					0.94	0.16	2.0
		0.0*	0.02	16.7	0.0*	0.02	4.0
Random tube (A5)	<i>a, b</i>	0.096	–	6.9	0.09	–	0.9
Straight tube (A7)	<i>a, b</i>	0.25	–	22.0	0.15	–	5.4

* *b* is set equal to zero (see text)

† Δ^2 = mean square difference between theory and data per data point. (Values are comparable between models but not between columns since they depend on the unscaled values of f^*)

errors, Δ^2 , to two of the data sets are shown in Table 1 for numerical comparison.

For the hoop model a direct best fit procedure yields a negative value for the coefficient *b*. This corresponds to a negative number of network chains and is thus physically meaningless. The best fit (plotted in Figure 2) which is physically acceptable is achieved by setting $b=0$ corresponding to a modulus which is independent of crosslink density. This is clearly a serious failing of the model. It does however, at least suggest that the number of entanglements per chain is large, and that entanglements dominate the elasticity. The fact that different data sets should superimpose so closely when scaled also indicates that the entanglement contribution to the stress is dominant.

In the replica slip-link model $b/a = N_c/N_s$, the ratio of number of crosslinks to slip-links. This is found to be somewhat less than 1 in all cases, implying slip-links are more important than crosslinks but not completely dominating. The stress contribution due to entanglements in the model is very sensitive to the value of η , making the function difficult to deal with numerically and not always yielding a unique best fit. For example, Table 1 shows that two almost equally good fits to the poly(dimethylsiloxane) (PDMS) data were obtained with very different parameter values. One of the η values, 0.64, implies that a slip-link can slide a distance several times the mean distance between slip-links. The other value, 0.16, represents a rather more restricted ability to slip. Worse fits were obtained at intermediate η . Since the hoop model suggests that the cross-link term is negligible ($b=0$) we also fitted the replica slip-link model using $b=0$. A rather poor fit was obtained, as judged by the Δ^2 value in Table 1, and the η was found to be very small (we note however, that while this is very different from the η obtained using the full three-parameter formula similarly small values ($\eta \approx 0.05$) were also obtained in a study of polybutadiene networks by Hvidt¹⁶). Such a small value implies that the slip-links were almost fixed in position along the chain contours. Finally we note that other experimental studies have found $\eta=0.4$ (polyisoprene¹⁷) and $\eta=1.1$ (polyethylene¹⁸). There is thus no consensus at all on the value of η obtained by various data fits. We therefore conclude that whilst the full three-parameter replica model provides a reasonable fit to many experimental data, the physical interpretation of the fitted values of the parameters N_c , N_s , and especially η is unclear and so must be viewed with extreme caution.

TUBE/LOCALIZATION MODELS

Of the several versions of the tube model that have been proposed, the most empirically successful is the localization model of Gaylord and Douglas¹⁰. The free energy (equation (A5)) consists of two terms: one is due to chain connectivity and has the Gaussian form, and is proportional to the number of crosslinks; another term represents the loss of degrees of freedom of the segments in the chains due to their spatial localization resulting from entanglements and packing. The magnitude of the localization or constraint parameter in the undeformed network ξ_0 is determined by representing the localization effect with a tube which is along the chain contour and has a length proportional to the chain contour length. The tube effectively represents the hard core volume of the chain, which is the ultimate physical basis for the chains being prevented from crossing and resulting in entanglement and packing effects. It then follows from a space-filling tube argument¹⁰ that the localization free energy term is proportional to the square of the segment density and hence to the plateau modulus of the uncrosslinked polymer. The chains are assumed to deform affinely so that the connectivity term has the Gaussian phantom chain network form. The deformation dependence of the localization term is determined by recognizing that the random orientation of network chains in the undeformed state requires a random tube around each chain, then by coarse graining this random tube is separated into tube sections lying along the principal deformation axes. Since the hard core volume of a chain is strain invariant, it follows that the diameter of the tube sections change during a constant volume deformation so as to preserve tube section volume. We note there is also a logarithmic term in the random tube model¹⁰ which is not relevant in the constant volume deformations which we consider here.

The straight tube model of Marrucci¹¹ places each randomly oriented network chain in a straight tube. The tube length is that of the end-to-end chain vector and deforms affinely while the tube diameter is assumed to change so as to maintain the straight tube volume. It has been shown¹ that equation (A6) obtained by Marrucci¹¹ gives a worse fit to the data than the Gaylord–Douglas model. However, Marrucci uses several unacceptable mathematical approximations. For example, if the straight tube volume is preserved, then the diameter *d* should vary as $1/d^2 \sim \langle M \rangle$ rather than $\langle M^2 \rangle^{1/2}$ as is assumed by Marrucci. We thus test the exact straight tube result

given by equation (A7), rather than Marrucci's approximate result equation (A6) which does not (and need not) satisfy the Valanis–Landel separability condition.

In Figure 3 we plot the random tube model (equation (A5)) and the exact straight tube model (equation (A7)) using the best fit parameters to the Rivlin and Saunders data¹² given in Table 1. The fit of the random tube model is comparable to that of the replica slip-link and the hoop models, giving a much better Δ^2 value for PDMS and a worse value for natural rubber. The exact straight tube model works considerably worse than any of these other three models in both cases and is not much of an improvement over the fit obtained using the corresponding approximate expression.

DISCUSSION

The random tube model, the replica slip-link model and the hoop model all predict that the modulus contains a term which is proportional to the square of the segment density ρ^2 and thus the plateau modulus. Another term in these models increases linearly with the crosslink density. This is found to be the case experimentally, for example in polybutadiene networks¹⁹ and ethylene–propylene copolymer networks²⁰. Whilst the modulus extrapolates smoothly to the plateau modulus of the uncrosslinked system as the crosslink density is decreased, the large deformation behaviour of entanglements leads to an entirely different stress–strain behaviour in the melt, where entanglements are transient, than in the corresponding network where the entanglements are permanent.

The data used above was chosen from the relatively small number of experiments which measure stress in both compression and extension on the same samples. It is well known that if extension alone is considered the data can be well represented by the phenomenological Mooney–Rivlin equation.

$$f^* = 2C_1 + 2C_2/\lambda$$

Fitting the straight line Mooney–Rivlin behaviour in extension is not a sufficiently stringent test for models having two or three parameters¹. It has been shown that the replica slip-link model provides good fits for several

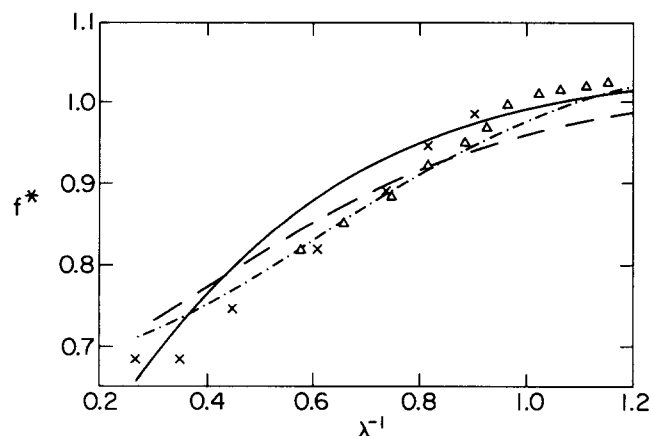


Figure 4 Mooney–Rivlin plot of the extension and small compression region. Data is from Figure 2. Theoretical curves are for: —, random tube model (equation (A5)); ---, hoop model (equation (A2)); - · - · -, replica slip-link model (equation (A4)). The fitting parameters were taken from Figures 2 and 3 and are based on fitting the entire data range rather than the more limited range shown (f^* units are kg cm^{-2})

experiments in extension only^{16–18}. In Figure 4 we plot the region $\lambda^{-1} \leq 1.2$ on an expanded scale. The same fitting parameters are used as in Figures 2 and 3, i.e. they are the best fits over the whole range of λ , not just for extension. Agreement is fair, although not particularly good when viewed on this scale. The replica slip-link model appears to give the best fit in this region, although Δ^2 values for the whole range are no better than those of the random tube and the hoop models (we note that the random tube model can produce Mooney–Rivlin behaviour exactly by choosing the tube diameter to deform affinely¹⁰).

Although the Mooney–Rivlin coefficients have no direct physical interpretation, we may use them to indicate whether entanglements yield a significant proportion of the stress in a network. On the scaled Mooney–Rivlin plots the gradient of the apparent straight line in extension is $g = C_2/(C_1 + C_2)$. For a phantom chain network $g = C_2 = 0$. Values of g calculated from published Mooney–Rivlin coefficients (e.g. 15, 17–20) cluster in the range 0.3–0.43. The trend is towards increasing g with increasing length of chain between crosslinks, i.e. increasing number of entanglements between crosslinks. This point has been discussed more fully elsewhere²¹. The upper limit of 0.43 ± 0.02 appears to be fairly constant in many materials, and corresponds to a network in which the entanglement contribution to stress dominates the crosslink contribution.

Finally we should note the elegant experiments of Batsberg and Kramer^{22,23} and Hvidt¹⁶ in which crosslinks are added to a melt which is frozen in a strained state. Entanglement effects are demonstrated unambiguously without recourse to any particular theory.

We wish to emphasize the broad consensus of experimental and theoretical ideas. Remaining discrepancies are at the level of a few per cent. The simple concepts of slip-links, hoops, localization and tubes have all had surprising success at modelling the complex nature of topological entanglements.

CONCLUSIONS

A wealth of experimental evidence clearly demonstrates the importance of the entanglement contribution to the stress behaviour of a polymer melt and its rather significant carryover to the stress–strain behaviour of the polymer when it is crosslinked into a network.

Data from a wide range of synthetic and natural rubbers can be closely superimposed in a scaled form.

The three models giving best fits to the data are the localization or random tube model, the hoop model and the replica slip-link model. None of these models provides an entirely satisfactory description of the data at a detailed level, but the discrepancies should not be allowed to obscure the good qualitative agreement between experiment and theoretical ideas.

ACKNOWLEDGEMENTS

P. G. Higgs is grateful for the support of the Agricultural and Food Research Council and Unilever Research. R. J. Gaylord benefited from continuous arguments with J. F. Douglas and has enjoyed the enthusiasm of G. B. McKenna. This work was supported in part, by a grant from the Polymer Program of the National Science Foundation.

REFERENCES

- 1 Gottlieb, M. and Gaylord, R. J. *Polymer* 1983, **24**, 1644
- 2 Doi, M. and Edwards, S. F. *J. Chem. Soc. Faraday Trans. II* 1978, **74**, 1789
- 3 Marrucci, G. *Rheol. Acta* 1979, **18**, 193
- 4 Graessley, W. W. *Adv. Polym. Sci.* 1982, **46**, 67
- 5 Higgs, P. G. and Ball, R. C. *Europhys. Lett.* 1989, **8**, 357
- 6 Kosc, M. *Colloid Polym. Sci.* 1988, **266**, 105
- 7 Adolf, D. *Macromolecules* 1988, **21**, 228
- 8 Ball, R. C., Doi, M., Edwards, S. F. and Warner, M. *Polymer* 1980, **22**, 1010
- 9 Edwards, S. F. and Vilgis, T. *Polymer* 1986, **27**, 483
- 10 Gaylord, R. J. *Polym. Bull.* 1982, **8**, 325; Gaylord, R. J. and Douglas, J. F. *Polym. Bull.* 1987, **18**, 347; Gaylord, R. J. and Douglas, J. F. in preparation
- 11 Marrucci, G. *Macromolecules* 1981, **14**, 434
- 12 Rivlin, R. S. and Saunders, D. W. *Proc. R. Soc. A* 1951, **243**, 251
- 13 Pak, H. and Flory, P. J. *J. Polym. Sci., Polym. Phys. Edn.* 1979, **17**, 1845
- 14 Treloar, L. R. G. *Trans. Faraday Soc.* 1944, **40**, 59
- 15 Erman, B. and Flory, P. J. *J. Polym. Sci., Polym. Phys. Edn.* 1978, **16**, 1115
- 16 Hvidt, S. *Proc. Networks 88*, Freiburg, September 1988
- 17 Thirion, P. and Weil, T. *Polymer* 1984, **25**, 609
- 18 Brereton, M. G. and Klein, P. G. *Polymer* 1988, **29**, 970
- 19 Dossin, L. M. and Graessley, W. W. *Macromolecules* 1979, **12**, 123
- 20 Pearson, D. S. and Graessley, W. W. *Macromolecules* 1980, **13**, 1001
- 21 Higgs, P. G. and Ball, R. C. in 'Physical Networks' (Eds W. Burchard and S. B. Ross-Murphy), Elsevier, Amsterdam, in press
- 22 Batsberg, W. and Kramer, O. *J. Chem. Phys.* 1981, **74**, 6507
- 23 Batsberg, W. in 'Biological and Synthetic Polymer Networks' (Ed. O. Kramer), Elsevier, Amsterdam, 1986, p. 509

APPENDIX A

Free energy expressions for various models in terms of the affine deformation relation M for uniaxial extension-compression.

Slip-link model³

$$F = a \langle M \rangle^2 \quad (\text{A1})$$

Hoop model⁵

$$F = a(\langle M \rangle^2 + \langle \ln M \rangle) + \frac{3}{2}b \langle M^2 \rangle \quad (\text{A2})$$

Hoop model⁷

$$F = a \ln \langle M^2 \rangle + b \langle M^2 \rangle \quad (\text{A3})$$

Replica slip-link model⁸

$$F = a \frac{1}{2} \sum_i \left(\frac{(1+\eta)\lambda_i^2}{1+\eta\lambda_i^2} + \ln(1+\eta\lambda_i^2) \right) + \frac{3}{2}b \langle M^2 \rangle \quad (\text{A4})$$

Random tube or Localization model¹⁰

$$F = a \left(\frac{\lambda + 2\lambda^{-1/2}}{3} \right) + \frac{3}{2}b \langle M^2 \rangle \quad (\text{A5})$$

Straight tube model¹¹

$$F = a \langle M^2 \rangle^{1/2} + \frac{3}{2}b \langle M^2 \rangle \quad (\text{approximate form}) \quad (\text{A6})$$

$$F = a \langle M \rangle + \frac{3}{2}b \langle M^2 \rangle \quad (\text{exact form}) \quad (\text{A7})$$

APPENDIX B

Functions of the affine deformation relation M appearing in Appendix A in terms of the uniaxial extension-compression deformation ratio λ .

$$M = \left(\frac{1}{\lambda} + \left(\lambda^2 - \frac{1}{\lambda} \right) \cos^2 \theta \right)^{1/2}$$

$$\langle M^2 \rangle = \frac{1}{3} \left(\lambda^2 + \frac{2}{\lambda} \right)$$

If $\lambda \geq 1$

$$\langle M \rangle = \frac{\lambda}{2} + \frac{\sinh^{-1} x}{2\lambda^{1/2} x}$$

where $x \equiv +(|\lambda^3 - 1|)^{1/2}$

$$\langle \ln M \rangle = \ln \lambda - 1 + \frac{\tan^{-1} x}{x}$$

If $\lambda < 1$

$$\langle M \rangle = \frac{\lambda}{2} + \frac{\sin^{-1} x}{2\lambda^{1/2} x}$$

where $x \equiv +(|\lambda^3 - 1|)^{1/2}$

$$\langle \ln M \rangle = \ln \lambda - 1 + \frac{\tanh^{-1} x}{x}$$